Supporting Information

Di-isopropyl ether assisted crystallization of organic-inorganic perovskites for efficient and reproducible perovskite solar cells

Lu-Yao Wang,[a] Lin-Long Deng,[*a] Xin Wang,[a] Tan Wang,[b] Hao-Ran Liu,[a] Si-Min Dai,[b] Zhou Xing,[b] Su-Yuan Xie, [*b] Rong-Bin Huang,[b] and Lan-Sun Zheng[b]

[a]*Pen-Tung Sah Institute of Micro-Nano Science and Technology, Xiamen University, Xiamen 361005, China. E-mail: denglinlong@xmu.edu.cn*

[b]*State Key Lab for Physical Chemistry of Solid Surfaces, iChEM (Collaborative Innovation Center of Chemistry for Energy Materials), Department of Chemistry, College of Chemistry and Chemical Engineering, Xiamen University, Xiamen 361005, China. E-mail: syxie@xmu.edu.cn*

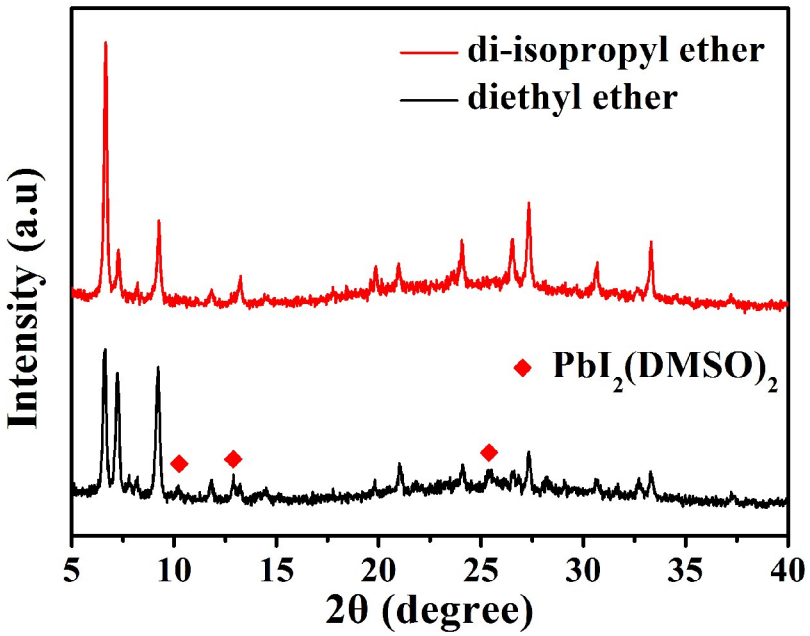

Fig. S1. XRD patterns of MAI-PbI_2-DMSO intermediate phase powders obtained by di-isopropyl ether or diethyl ether treatment.

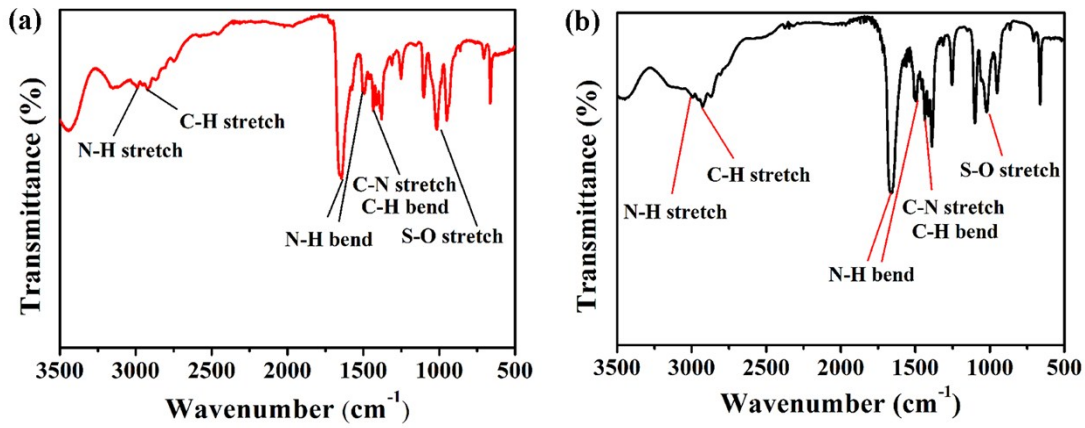

Fig. S2. FTIR spectra of the MAI-PbI_2-DMSO intermediate phase powders obtained by (a) di-isopropyl ether, and (b) diethyl ether treatment.

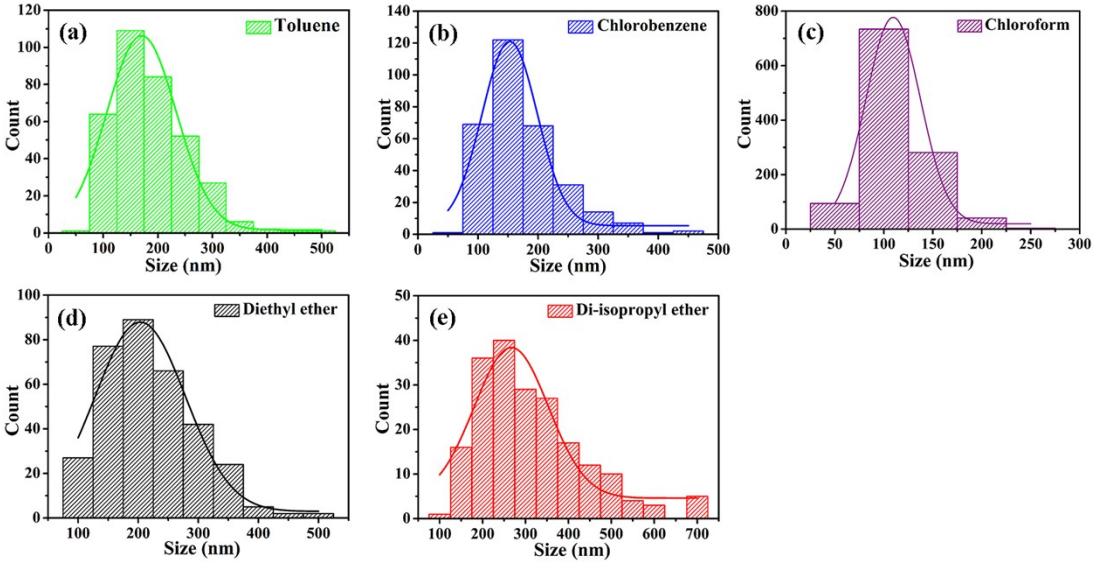

Fig. S3. Grain size distributions of the perovskite films estimated from the SEM images using Nano Measurer software.

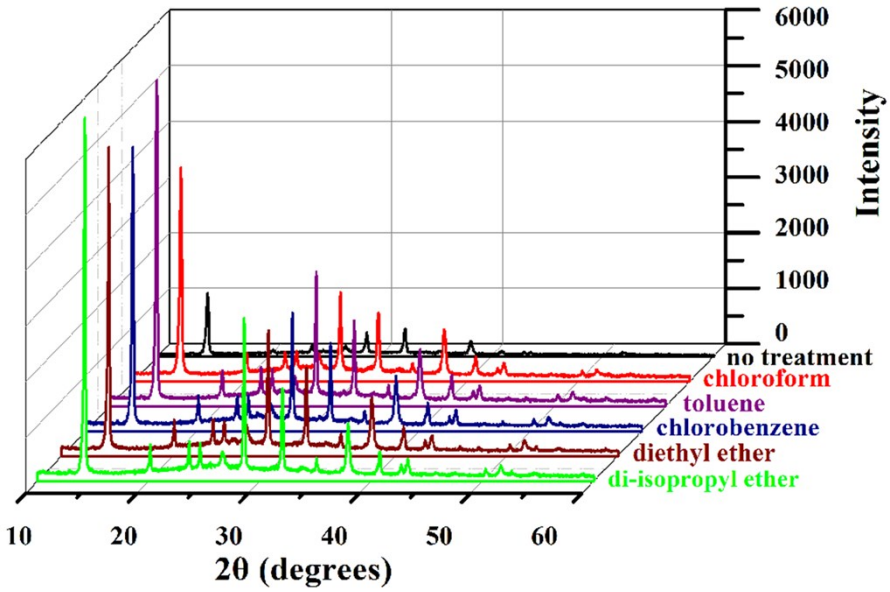

Fig. S4. XRD patterns of perovskite films prepared by anti-solvent deposition method without and with different anti-solvent treatment.

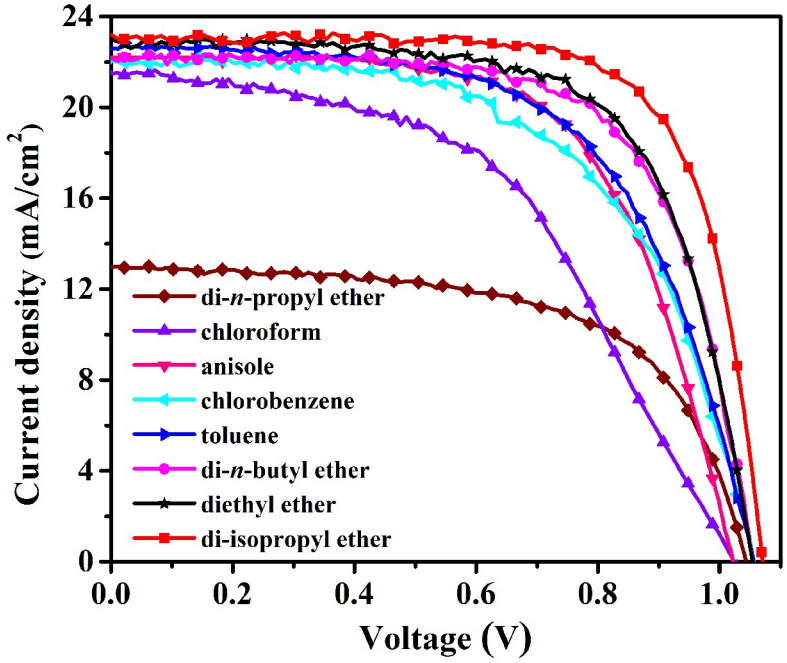

Fig. S5. *J-V* curves of perovskite solar cells fabricated with different anti-solvent treatment. The *J-V* data were collected in the reverse scan under AM 1.5G 100 mW cm^{-2} illumination.

Table S1. Photovoltaic parameters of perovskite solar cells fabricated with different anti-solvent treatment. The statistical data are determined from 10 devices.

Solvent	V_{oc} (V)	J_{sc} (mA/cm^2)	FF (%)	PCE (%)
di-*n*-propyl ether	1.04 ± 0.01	13.19 ± 2.11	58.07 ± 3.69	7.96 ± 1.61
chloroform	1.02 ± 0.05	21.59 ± 0.95	50.46 ± 2.55	11.11 ± 0.43
anisole	1.02 ± 0.01	22.00 ± 0.56	63.71 ± 2.54	14.26 ± 0.75
chlorobenzene	1.05 ± 0.03	22.12 ± 1.55	62.28 ± 2.03	14.51 ± 0.65
toluene	1.06 ± 0.04	22.56 ± 1.52	63.82 ± 4.08	15.25 ± 1.56
di-*n*-butyl ether	1.06 ± 0.02	22.60 ± 0.58	66.75 ± 2.54	15.99 ± 0.88
diethyl ether	1.06 ± 0.02	22.70 ± 1.07	67.75 ± 3.38	16.26 ± 0.88
di-isopropyl ether	1.07 ± 0.01	22.90 ± 0.71	72.42 ± 2.91	17.19 ± 0.52

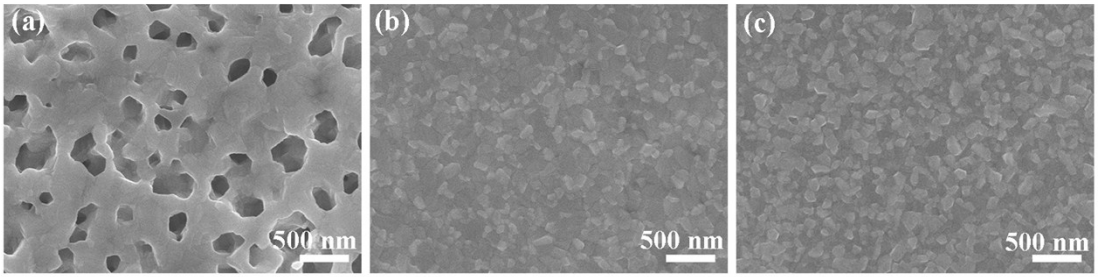

Fig. S6. Top view SEM images of perovskite films prepared by anti-solvent deposition method with different solvent treatment: (a) di-*n*-propyl ether, (b) di-*n*-butyl ether, and (c) anisole.

Table S2. Parameters of the time-resolved photoluminescence spectra of perovskite films fabricated under different annealing temperatures.

Temperature (°C)	τ_{ave} (ns)	τ_1 (ns)	Amplitude of τ_1 (%)	τ_2 (ns)	Amplitude of τ_2 (%)
80	35.8	2.89	44.86	37.80	55.14
100	51.6	3.92	33.83	53.38	66.17
120	46.7	2.89	35.31	48.15	64.69
150	24.2	4.50	59.37	28.69	40.63

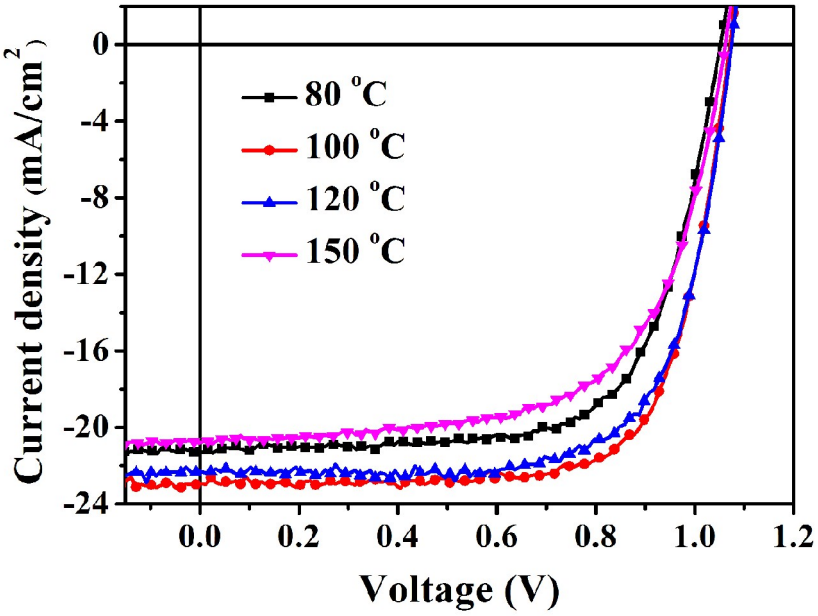

Fig. S7. *J-V* curves of perovskite solar cells with different pre-annealing temperatures. Devices were fabricated with $CH_3NH_3PbI_3$ film prepared by di-isopropyl ether treatment. The *J-V* data were collected in the reverse scan under AM 1.5G 100 mW cm^{-2} illumination.

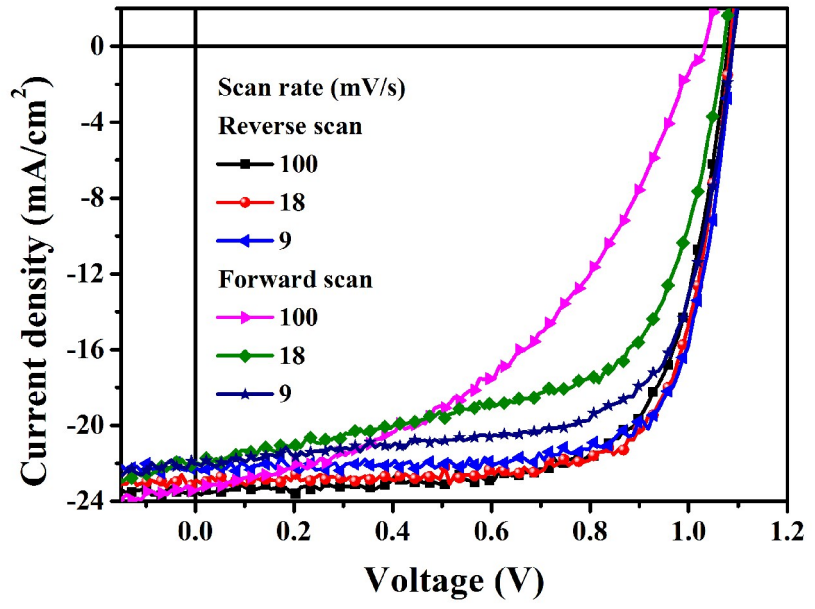

Fig. S8. *J-V* curves of perovskite solar cells measured with different scan rates and different scan directions with $CH_3NH_3PbI_3$ film prepared by di-isopropyl ether treatment. The measurements were carried out under AM 1.5G 100 mW cm^{-2} illumination.

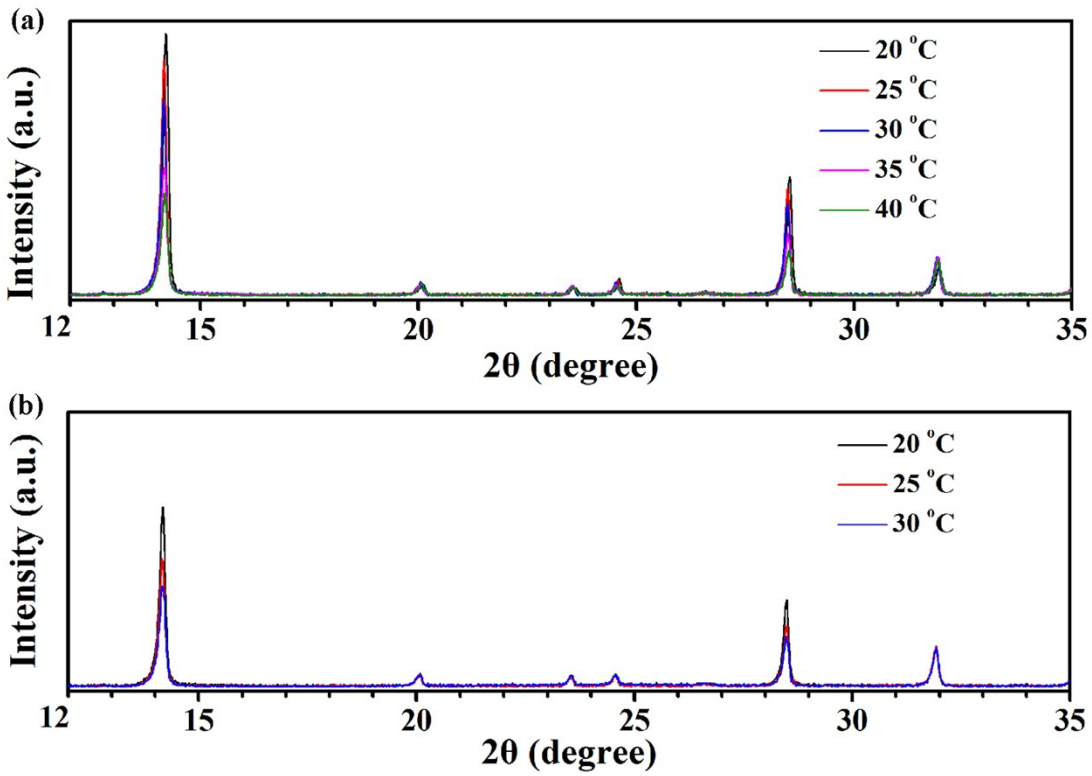

Fig. S9. XRD patterns of perovskite films treated with (a) di-isopropyl ether or (b) diethyl ether at different ambient temperatures.

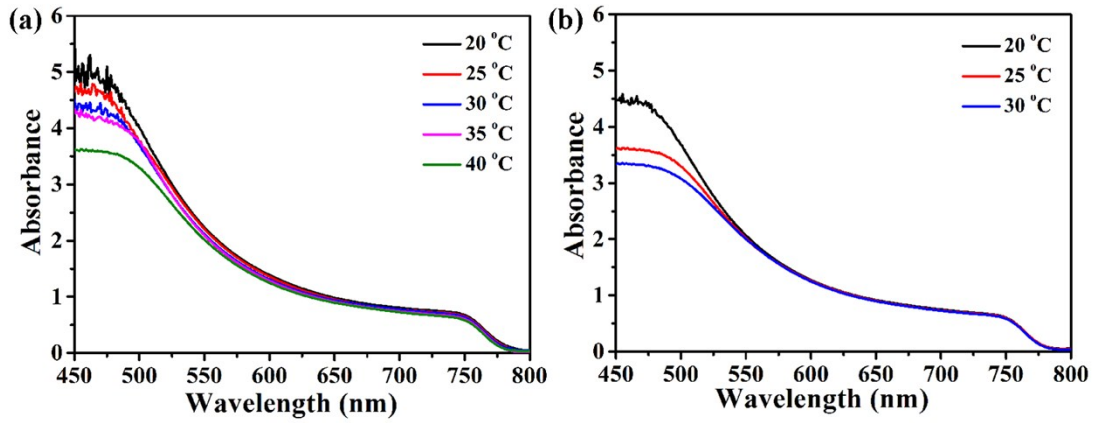

Fig. S10. UV-Vis absorption spectra of perovskite films treated with (a) di-isopropyl ether or (b) diethyl ether at different ambient temperatures.

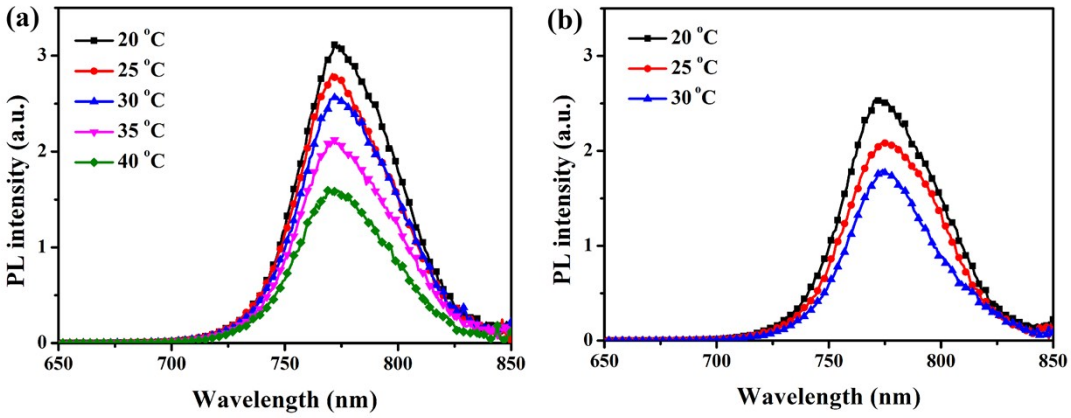

Fig. S11. PL spectra of $CH_3NH_3PbI_3$ layer deposited on mesoporous TiO_2 substrate treated with (a) di-isopropyl ether or (b) diethyl ether at different ambient temperatures.